Radio Science, Volume 36, Number 1, Pages 45–51, January–February 2001

Antenna compression using binary phase coding

Ronald F. Woodman and Jorge L. Chau[1]

Radio Observatorio de Jicamarca, Instituto Geofísico del Perú, Lima, Peru

Abstract. We introduce the first antenna "compression" scheme for coherent radars. The idea is to transmit with a large array of phase-coded antennas at full power and later synthesize by linear superposition and proper phasing, the equivalent of a small transmitting antenna, similar to a single antenna module of the array. The full "decoding" is done by software by adding the power and cross-power estimates of the signals of each code, so no extra burden is added other than the summations. This approach allows the use of all the available power in phased array systems where either high-power transmitters cannot be used with small antennas or the transmitted power is distributed among the antenna elements. The wider beams are particularly important in meteor systems and, recently, in some radar studies of the neutral atmosphere, especially when multiple receiving antennas are used. Our scheme is based on complementary binary phase coding of antenna elements and works in a similar fashion to complementary phase coding used in pulse compression. We have implemented this idea at the Jicamarca Radio Observatory using a two-dimensional approach; thus four two-dimensional complementary codes were derived. The performance of this implementation has been tested using imaging techniques on an interferometer of four receiving antenna modules to study the angular characteristics of the well-known equatorial electrojet irregularities. In addition, in this mode we have made successful observations of the upper troposphere and lower stratosphere.

1. Introduction

Until recently, most applications of coherent radars require a very narrow beam, particularly when only one receiving antenna is used, to simplify the interpretation of the returned signals. For example, in mesosphere-stratosphere-troposphere (MST) radars, narrower beams are preferred to avoid the effects of beam-broadening on turbulence measurements [e.g., *Chau et al.*, 2000, and references therein], the spatial inhomogeneities in velocity measurements [e.g., *Kudeki et al.*, 1993], or multiple meteors in meteor detection systems [e.g., *Nakamura et al.*, 1991]. However, these unwanted effects related to the use of wider transmitting beams are overcome, and more applications are found to wide transmitting beams when they are complemented with multiple receiving antennas and radar interferometry/imaging techniques.

In phase arrays one can get the widest beam possible by transmitting in one of the antenna modules. Furthermore, one would like also to be able to use all the high power usually available with the big antenna, which is not usually possible because of the maximum power limitations of a single module. This problem is obvious if one has a phased array with a single high-power transmitter (e.g., the Jicamarca incoherent scatter radar), where the total high power cannot be transmitted with single antenna elements. A similar problem is present if one has a phased array with distributed transmitters (e.g., the middle and upper atmosphere (MU) VHF radar in Japan or the Buckland Park MF radar in Australia).

In this paper we present a solution to overcome this limitation, i.e., how to transmit a wide beam and all the available power. Our scheme is based on complementary binary phase coding of the antenna elements in a similar fashion to phase coding used in pulse compression [e.g., *Farley*, 1985a]. We trans-

[1]Also at Laboratorio de Física, Universidad de Piura, Piura, Peru.

Paper number 2000RS002388.
0048-6604/01/2000RS002388$11.00

mit an evenly distributed power in each phase-coded module. Complementary phase-coded schemes are sent in succession. After "decoding," the end result is equivalent to having sent all the power in a single module. Decoding is performed by software by simply adding the power and cross-power estimates of each of the coded signals. Therefore no extra burden is added to the processing other than a few summations.

One application of antenna compression schemes is in radar interferometer/imaging experiments of the neutral atmosphere, where broader beams and high power are needed in order to cover the whole aspect-sensitive region or to see atmospheric structures that are broader than the narrow beams usually used by most MST radars. Recent radar images of the lower atmosphere have shown that the aspect sensitivity function and structure of the atmosphere usually extend beyond the relatively narrow (less than 5°) field of view of typical MST radars [e.g., *Worthington et al.*, 1999a, 1999b; *Chau and Woodman*, 2000; *Hélal et al.*, 2000]. Another application is in the detection and observation of meteor trails. In this case, the use of wider beams and high power would allow the observation of a larger number of meteors with larger horizontally projected velocities.

We have tested the feasibility of antenna compression at Jicamarca by performing imaging experiments of the equatorial electrojet (EEJ) and the upper troposphere and lower stratosphere. The angular characteristics of the EEJ irregularities are well known [e.g., *Farley*, 1985b; *Kudeki and Farley*, 1989], so we use them to evaluate the performance of our implementation. In section 2 we present the details of the derivation and the implementation of the codes used at Jicamarca. The experimental results are presented in section 3. Finally, the main conclusions are summarized in section 4.

2. Experimental Setup

Following the analogy to pulse compression, where a long coded pulse is transmitted and later synthesized into a narrow pulse with the same total energy, we have derived a set of codes that allow us to transmit with a coded antenna of large dimensions so that one can later synthesize a small antenna (wide beam) with an equivalent transmitted power.

An easy way to think about the analysis is to use the concept that the antenna power pattern (or angular spectrum) is the Fourier transform (in the far field) of the spatial autocorrelation function (ACF) of the aperture electric field distribution. The idea is to transmit different coded ACF patterns. A good code will generate a spike at zero displacement and some smaller sidelobes at other displacements in the ACF. The complementary nature of the codes we have derived allows us to remove such sidelobes.

In the spectral angular domain the beam pattern of each coded antenna will be wider than without the use of code; however, the resulting beam is not smooth. We should recall that power at large autocorrelation displacements transforms into small angular structure. A smooth beam is obtained when we remove the ACF sidelobes by the complementary nature of the codes. These ideas will become clearer as we describe one particular implementation.

Four two-dimensional complementary codes are obtained from the four possible combinations of the outer products of the two one-dimensional codes C = [1,1,1,-1] and C′ = [1,1,-1,1], i.e., from $C_x \otimes C_y$, $C_x \otimes C'_y$, $C'_x \otimes C'_y$, and $C'_x \otimes C_y$ (where circled times symbol stands for outer product). The four result-

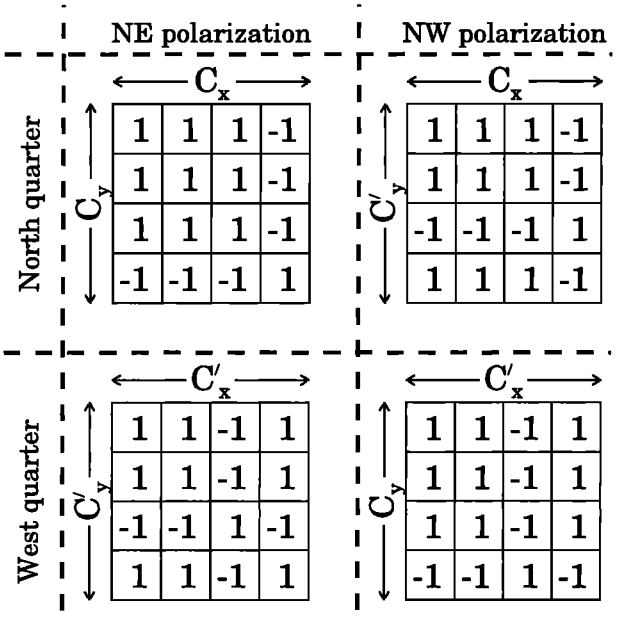

Figure 1. Four complementary binary codes of 4 x 4 elements. These codes have been obtained from the different combinations of the complementary codes C = [1,1,1,-1] and C′ = [1,1,-1,1]. Using the Jicamarca antenna, codes CC and C′C′ have been implemented with two quarters of the NE polarization, and codes CC′ and C′C have been implemented with two quarters of the NW polarization, respectively.

ing two-dimensional codes are depicted in Figure 1 for our specific example. We will refer to them as CC, CC′, C′C′, and C′C for short. Here we have used four element codes, but codes of more elements can be attained in a similar way by combining complementary codes of more bits [e.g., *Gonzales and Woodman*, 1984]. Note that when the antenna compression is needed only in one dimension (e.g., studies of field-aligned irregularities), one needs to use only a simple sequence of one-dimensional complementary codes (i.e., codes C and C′). As in pulse compression, "1" represents a 0° phase shift, and "-1" represents a 180° phase shift.

In Figure 2 we show the spatial ACF of each of the coded antennas. Since the ACFs are symmetric with respect to the each of the dimensions, we show only the positive lags in both dimensions. Note the complementary nature of the ACFs; by adding all of them we obtain a spike at zero lag without any sidelobes.

Note that in contrast to the pulse compression technique we do not need to decode by cross-correlating the signal with the code itself. Since the beam pattern is the Fourier transform of the spatial ACF of the aperture electric field distribution, the autocorrelation operation and therefore the decoding are performed naturally. This justifies our use of the word "decoding" between quotes in the abstract and several places in the text. There are no extra computations needed beyond the evaluation of the power and cross-power estimates. The suppression of the ACF sidelobe characteristics of the complementary codes is achieved by adding once the four independent estimates of power and cross-power at the end of an integration cycle.

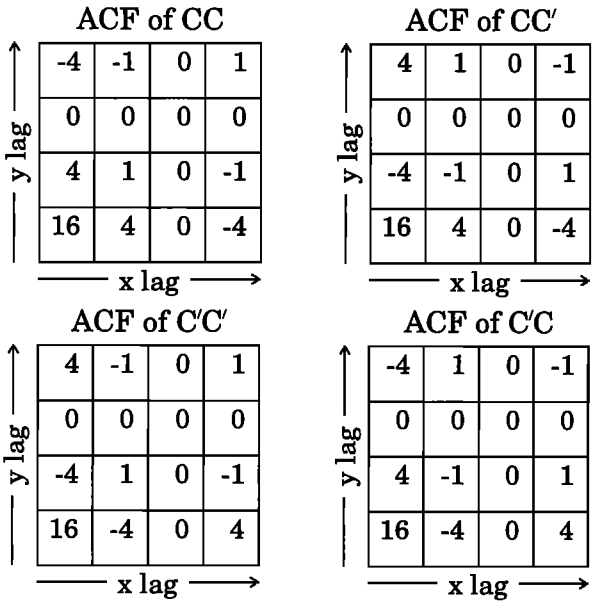

Figure 2. Spatial autocorrelation functions of each of the coded antennas. Note that there is a peak at zero lag on all ACFs (lower left corner) and minor sidelobes at other lags. After adding all the ACFs all the sidelobes are removed.

Normally, we should have implemented the four different codes of the 4 x 4 elements of a quarter array from pulse to pulse. Since pulse-to-pulse phase switching is not possible at Jicamarca, we have accomplished the same by prewiring four arrays of 4 x 4 antenna modules (quarters) with the corresponding phase codes. The four prewired quarters consist of two quarters (north and west) of two orthogonal polarizations each. The two polarizations are transmitted simultaneously, and their independence is confirmed by their being received in the two polarizations of whatever receiving system is used. The north and west quarters are transmitted consecutively with full power each. The full power switching is accomplished by feeding the two transmitters used (1 MW each) into a hybrid. By feeding one of the transmitters with the same or opposite phase of the other, the full power is output into either of the two outputs of the hybrid connected to the north and west quarters. The phase switching is accomplished at the low-power excitation level. In other words, we do not "compress" the full 8 x 8 module array. Compression of the 4 x 4 subarrays is sufficient.

We have used such a transmitting configuration in an imaging experiment. For reception we used the imaging configuration shown in Figure 3. We used four receiving elements (A, B, C, and D) consisting of two polarizations each. Therefore there were eight receiving antenna modules, four using the NE polarization and four using the NW polarization. Raw data were recorded for later processing.

The one-way antenna patterns of the coded quarter sections are shown in Figure 4. In addition, in Figure 4e we show the antenna pattern obtained after adding the power of each of the coded patterns. This resulting pattern is equivalent to the pattern of a single antenna module, as expected. Note that the beam patterns of each of the coded antennas are already wide but not smooth because of the sidelobes in the spatial ACFs. In some applications, e.g., me-

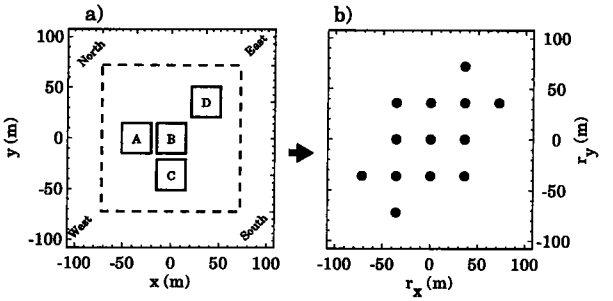

Figure 3. (a) Receiving array and (b) its corresponding visibility domain (points of the spatial autocorrelation function that are sampled). Each of the receiving elements consists of two collocated antennas using orthogonal polarizations. The dashed square represents the size of the quarter sections used for transmission.

teor detection, a smooth transmitting beam is not necessary, and one could use any of the codes or other codes to make the beam wider [e.g., *Nakamura et al.*, 1991]. Imaging, on the other hand, has much stronger requirements on the smoothness of the pattern.

The north and west antenna quarters are not collocated, but this separation has no effect for the resulting pattern in the far field (above 15 km). Below 15 km the resulting pattern is not perfectly symmetric, and there are some angular deviations (from the pattern of a module) along the direction of the antenna displacements (i.e., the west to north direction); however, these deviations are a fraction of a degree and could be considered negligible above ~7.5 km (far-field boundary for a quarter section).

The eight-antenna receiving system needs to be phase calibrated; for this we have used the EEJ echoes and a narrow transmitting beam pointing perpendicular to the magnetic field. After a long integration time (>1 min), EEJ echoes were processed, and the phase differences of the receiving elements of the system were calculated. This approach is feasible, given that we know the location of the centroid of the EEJ. A similar approach was used by *Chau and Woodman* [2000].

We have conducted basically two antenna compression experiments: (1) coded EEJ and (2) coded upper troposphere and lower stratosphere (ST). The basic parameters of these experiments are shown in Table 1. In order to obtain altitude resolution and take advantage of the maximum transmitter duty cy-

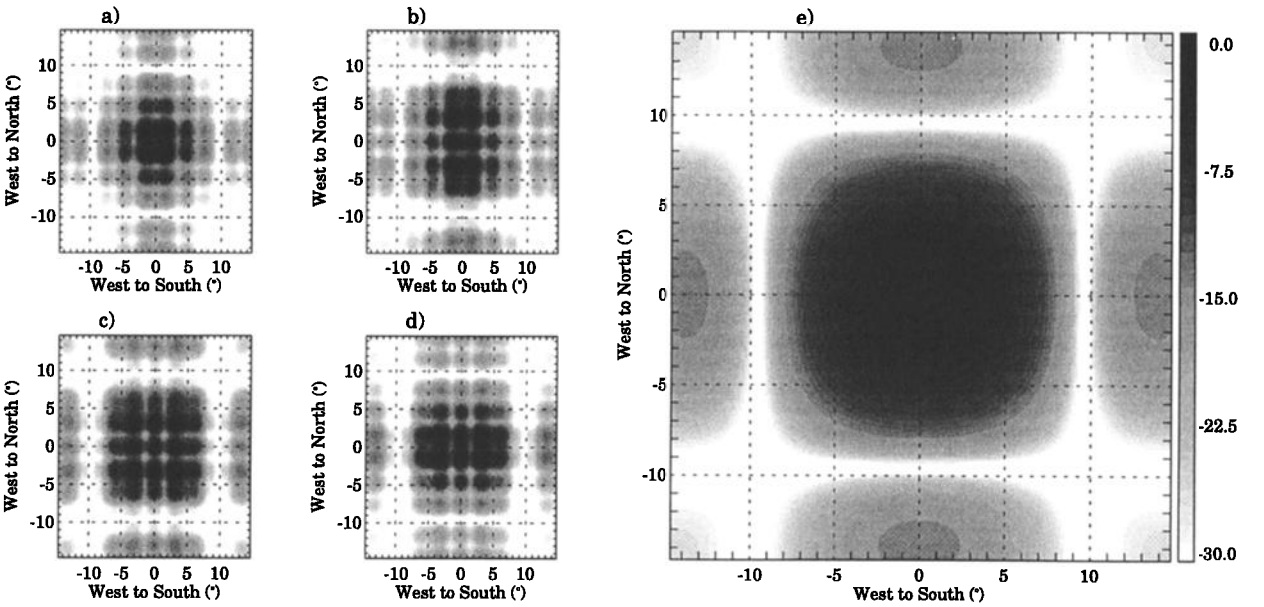

Figure 4. Theoretical one-way power patterns of quarter sections (i.e., 4 x 4 modules) of the Jicamarca antenna using codes (a) CC, (b) CC′, (c) C′C′, and (d) C′C, along with (e) the resulting pattern of adding all the coded ones. The resulting pattern is identical to the pattern of a single Jicamarca module. North is in the left-hand corner of each contour plot. The gray scale represents the levels of normalized power in decibels.

Table 1. Operating Parameters for the Antenna Compression Experiments Conducted at Jicamarca During November 26-27, 1999

Parameter	Coded EEJ	Coded ST
Duration	30 min	14 hours
Pulse repetition period	2.5 ms	2.5 ms
Delay[a]	1.25 ms	1.25 ms
Coherent integrations	2	50
Initial height	95 km	12 km
Altitude resolution	0.45 km	0.45 km
Number of heights	30	30
Pulse code	1	11100010010
Pulse width	0.45 km	4.95 km
Transmitting power	2 MW	2 MW
Transmitter beam width[b,c]	~8.1°	~8.1°
Transmitter beam position	on axis[d]	on axis
Receiver beam width[c]	~8.1°	~8.1°
Receiver beam position	on axis	on axis

[a]Between codes CC/C′C′ and CC′/C′C.
[b]Effective beam width after adding the four coded beams.
[c]One-way half-power beam width.
[d]The on-axis position is −1.46° from the true vertical in the SE direction.

cle to increase the signal sensitivity, we have pulse-coded the ST experiment with an 11-bit Barker code.

Note that the on-axis position is −1.46° from the vertical position in the SE direction. In section 3 the on-axis position is indicated by the center of all images (i.e., 0°,0°).

3. Experimental Results

In Figure 5 we show an example of two-dimensional images of the EEJ at 100.4 km obtained after 1 min integration. This experiment was performed mainly to test the performance of the system under predictable conditions. The long integration has been used so that any east-west structure in the scattering medium will be averaged out. Hence the brightness corresponds to the combined effect of the transmitting and receiving beams. These images were obtained using the maximum entropy (MaxEnt) algorithm [e.g., *Janes*, 1985] on the visibility samples, i.e., normalized complex cross-correlation values at zero lag. The MaxEnt algorithm maximizes the entropy of the assumed model, i.e., least number of assumptions beyond what we actually know. We have applied the algorithm presented by *Hysell* [1996], where the estimation of the brightness distribution reduces to solving a set of nonlinear equations.

Figures 5a, 5b, 5c, and 5d show the images obtained by processing the signals of each code independently. In Figure 5e we show the EEJ image

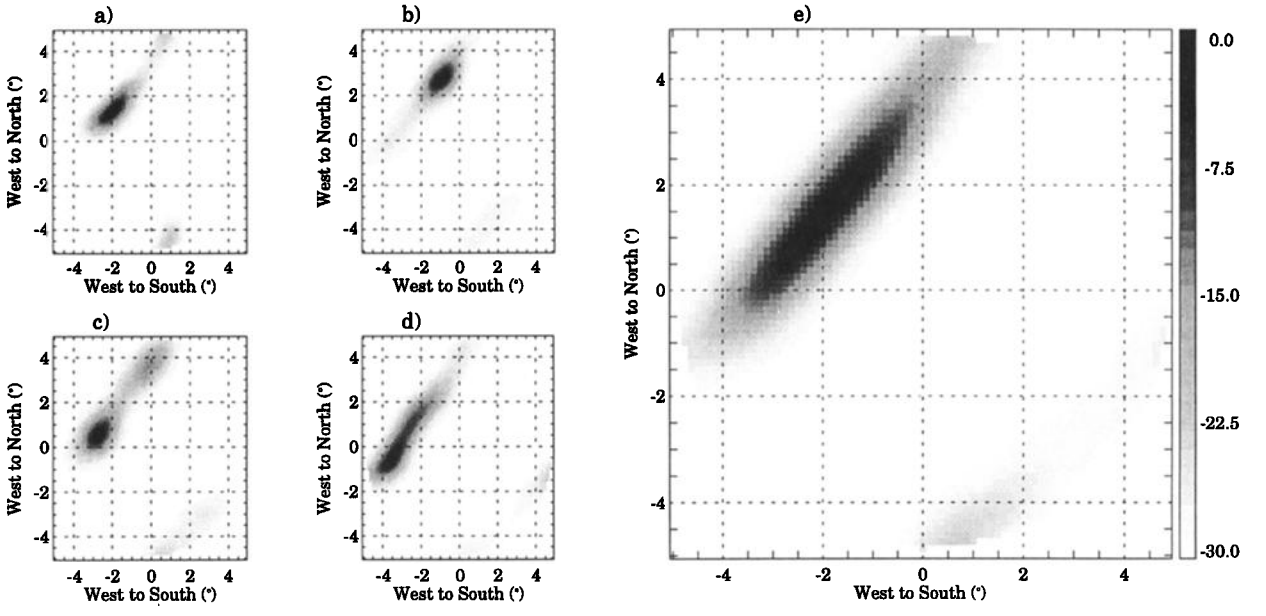

Figure 5. Two-dimensional normalized images of the EEJ at 100.4 km obtained after a 1 min integration, using codes (a) CC, (b) CC′, (c) C′C′, and (d) C′C and (e) adding the spatial ACF of all four codes. The images have been obtained using the maximum entropy method. The gray scale indicates the levels of brightness in decibels.

obtained from the sum of visibility functions of all codes. Each image has been normalized to unity in each plot. The gray scale indicates the normalized brightness in decibels.

Note that the resulting EEJ image (e.g., Figure 5e) is in very good agreement with what we expected, i.e., very aspect sensitive in the north-south direction and isotropic (limited by the transmitting and receiving antenna beam width) in the east-west direction. Moreover, if we multiply this EEJ image by the antenna pattern of each of the codes of Figure 4 (i.e., Figures 4a, 4b, 4c, and 4d), the resulting images are in reasonably good agreement with Figures 5a, 5b, 5c, and 5d, respectively. Note some angular aliasing at the bottom right of all panels, which is due to the receiving antenna spacing used.

Preliminary imaging results from the tropopause and lower stratosphere are presented in Figure 6. These images have been also obtained using the maximum entropy algorithm on the sum of the visibility samples of all codes after 3 min integration. These images have been also normalized to unity. The long integration in this case would allow us to see the aspect sensitivity (if present) of the echoes, if it is narrower than the broad beam used. Given that we have used wide transmitting and receiving beams, the brightness distribution we show is a good measure of the aspect sensitivity function as a function of angle.

Contrary to the tropospheric images presented by *Chau and Woodman* [2000], these images are very aspect sensitive (narrow angular distribution) and present continuity in height and also in time (results not presented). It is important to note that the transmitting and receiving antennas are pointing on axis, i.e., 1.46° off vertical in the north to west direction. This explains the offset in the west to north direction assuming that the structures are predominantly horizontal. The offset in the west to south direction is not the same from height to height and could be of geophysical nature (e.g., gravity waves with long wavelengths). The use of shorter integration times is currently under study in order to see if more geophysical information, other than the aspect sensitivity function, namely inhomogeneous turbulent structure, can be attained by using imaging techniques. We hope that by using the full transmitter power we should be able to see the structure of the stratospheric and mesospheric echoing regions.

4. Conclusions

We have described an innovative scheme to obtain a broad antenna pattern from a physically large antenna. The technique is analogous to pulse compression and allows the transmission of all the available transmitter power in phased array systems with very high power transmitters or with distributed transmitters.

At Jicamarca the implementation required the use of different antennas with prewired coded phases. However, this limitation can be overcome by other systems that are able to switch the antenna phases from pulse to pulse, where each code could be used on consecutive transmitter pulses.

We have implemented and tested only a sequence of complementary binary codes of 4 x 4 elements. Other sequences can be easily obtained using the properties of known codes following our procedure described in section 2, particularly if square or rectangular phase arrays are used.

It should be mentioned that an alternative scheme to broaden the transmitting beam consists of phase

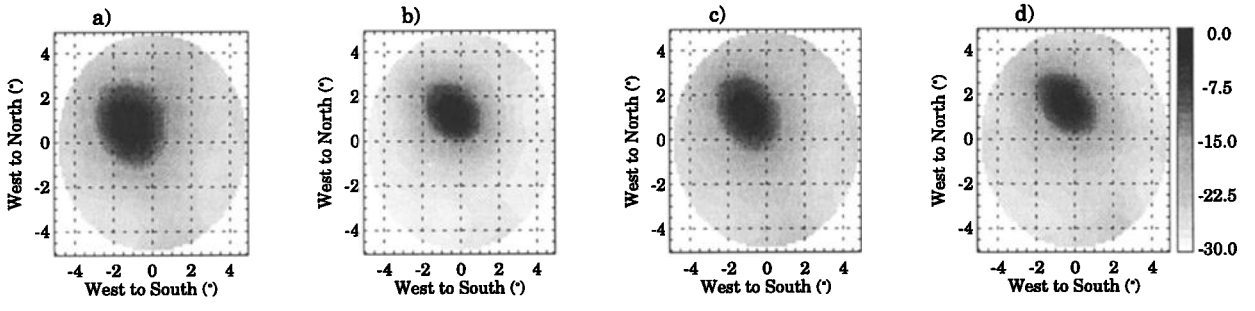

Figure 6. Two-dimensional normalized images of the tropopause and lower stratosphere heights after 3 min integration using maximum entropy in the sum of the visibility samples of all four codes: (a) 16.95 km, (b) 17.85 km, (c) 18.75 km, and (d) 19.65 km.

coding the array modules so that a spherical phase front corresponding to a point source below the antenna aperture is approximated. The technique has actually been implemented at Jicamarca by one of the authors (R. F. Woodman). It can be considered as another possible code, but a perfect match to a spherical phase front requires the implementation of an arbitrary phase on each module. Jicamarca and other phase arrays can switch only a discrete set of phases (only four at Jicamarca). Our complementary scheme requires only two, 0° and 180°, and achieves perfectly the pattern of a single module, which is the optimum possible for any other scheme.

The performance of our scheme has been tested by obtaining images of the EEJ after long integrations. The results were as expected, i.e., very aspect sensitive (very narrow) in the north-south direction and isotropic in the east-west direction, limited by the (single module) antenna beam width. Moreover, the images obtained by processing each code independently are in good agreement with the images resulting from the multiplication of the expected EEJ image and the theoretical patterns of each code.

As an application, we have made observations of the upper troposphere and lower stratosphere, and we have verified that the latter is more aspect sensitive than the lower troposphere. Further analysis of these lower atmospheric data is currently underway, mainly using shorter integrations, in order to decide on the benefits of applying imaging techniques to these lower regions.

Acknowledgments. We thank D. T. Farley for his careful reading of the original manuscript. The help of the Jicamarca staff (in particular M. Sarango) during the experimental setup is appreciated. The Jicamarca Radio Observatory is operated by the Geophysical Institute of Perú, with support from NSF Cooperative Agreement ATM-9408441. J.L.C. was supported by the National Science Foundation under agreement ATM-9813910.

References

Chau, J. L., and R. F. Woodman, Three-dimensional coherent radar imaging at Jicamarca: Comparison of different inversion techniques, *J. Atmos. Sol. Terr. Phys.*, *in press*, 2000.

Chau, J. L., R. J. Doviak, A. Muschinski, and C. L. Holloway, Tropospheric measurements of turbulence and characteristics of bragg scatterers using the Jicamarca VHF radar, *Radio Sci.*, *35*, 179–193, 2000.

Farley, D. T., On-line data processing techniques for MST radars, *Radio Sci.*, *20*, 1177–1184, 1985a.

Farley, D. T., Theory of equatorial electrojet plasma waves: New developments and current status, *J. Atmos. Sol. Terr. Phys.*, *47*, 729–744, 1985b.

Gonzales, C. A., and R. F. Woodman, Pulse compression techniques with application to HF probing of the mesosphere, *Radio Sci.*, *19*, 871–877, 1984.

Hélal, D., M. Crochet, H. Luce, and E. Spano, Radar imaging and high-resolution array processing applied to a classical VHF-ST profiler, *J. Atmos. Sol. Terr. Phys.*, *in press*, 2000.

Hysell, D. L., Radar imaging of equatorial *F* region irregularities with maximum entropy interferometry, *Radio Sci.*, *31*, 1567–1578, 1996.

Janes, E. T., *Where Do We Go Fom Here?*, chap. 2, pp. 21–58, D. Reidel, Norwell, Mass., 1985.

Kudeki, E., and D. T. Farley, Aspect sensitivity of equatorial electrojet irregularities and theoretical implications, *J. Geophys. Res.*, *94*, 426–434, 1989.

Kudeki, E., P. K. Rastogi, and F. Sürücü, Systematic errors in radar wind estimation: Implications for comparative measurements, *Radio Sci.*, *28*, 169–179, 1993.

Nakamura, T., T. Tsuda, M. Tsutsumi, K. Kita, T. Uehara, S. Kato, and S. Fukao, Meteor wind observations with the MU radar, *Radio Sci.*, *26*, 857–869, 1991.

Worthington, R. M., R. D. Palmer, and S. Fukao, Complete maps of the aspect sensitivity of VHF atmospheric radar echoes, *Ann. Geophys.*, *17*, 116–119, 1999a.

Worthington, R. M., R. D. Palmer, and S. Fukao, An investigation of tilted aspect-sensitive scatterers in the lower atmosphere using the MU and Aberystwyth VHF radars, *Radio Sci.*, *34*, 413–426, 1999b.

J. L. Chau and R. F. Woodman, Radio Observatorio de Jicamarca, Apartado 13-0207, Lima, Peru. (chau@geo.igp.gob.pe; ron@geo.igp.gob.pe)

(Received May 11, 2000; revised September 18, 2000; accepted October 19, 2000.)